Phonon dispersion of bcc La

F. Güthoff
Institut Laue-Langevin, Boîte Postale 165, F-38042 Grenoble CEDEX, France
and Institut für Metallforschung, Universität Münster, D-4400 Münster, Germany

W. Petry
Institut Laue-Langevin, Boîte Postale 165, F-38042 Grenoble CEDEX, France

C. Stassis
Ames Laboratory and Department of Physics, Iowa State University, Ames, Iowa 50011

A. Heiming
Institut Laue-Langevin, Boîte Postale 165, F-38042 Grenoble CEDEX, France

B. Hennion
Laboratoire Léon Brillouin, CEN Saclay, 91191 Gif-sur-Yvette CEDEX, France

C. Herzig
Institut für Metallforschung, Universität Münster, D-4400 Münster, Germany

J. Trampenau
Institut Laue-Langevin, Boîte Postale 165, F-38042 Grenoble CEDEX, France
(Received 20 July 1992)

The phonon-dispersion curves of the high-temperature bcc phase of La (γ-La) have been measured at 1163 K. A characteristic valley of transverse and low-energy phonons extends along the $[\xi\xi 0]$ and $[\xi\xi 2\xi]$ propagation directions. The eigenvectors of these modes are in the direction of the displacements needed for phase transitions to low-temperature close-packed structures. On the one hand they are indicative of the low potential barrier of the bcc phase for displacements toward these close-packed structures, whereas on the other hand the bcc structure is stabilized by the contribution of these low-energy modes to the lattice entropy. All these modes are strongly damped and have lifetimes of a few vibrational periods. Interference effects due to multiphonons can be the origin of the observed pronounced alterations of the one-phonon scattering law.

I. INTRODUCTION

All transition metals from group III to group VI solidify in a bcc structure. Those of groups III and IV are only stable at elevated temperatures with a particular narrow existence range in the group-III metals Sc, Y, and La. Whereas Sc and Y, like all group-IV metals, transform to the hexagonal close-packed structure, La has the unusual phase sequence bcc(γ)$\rightarrow$fcc(β)$\rightarrow$ double-hcp(α) with the melting point at 1191 K and the martensitic transitions at 1138 and 709 K, respectively. From all group-III metals, only La shows superconductivity with a relatively high transition temperature $T_c = 6.05$ K. As the first member of the rare-earth series of elements, an understanding of the properties of La is of particular importance because these properties are frequently compared with those of other rare earths with occupied $4f$ levels. Knowledge of the phonon dispersion of the different phases in La is certainly an elementary key to understand the physical properties of La.

Phonon dispersions have been measured in the fcc phase by Stassis *et al.*[1,2] The excess enthalpy of the β-to-α transition is low, so that fcc single crystals can easily be quenched to room temperature. This is not the case for the γ-to-β transition. The higher excess enthalpy and the martensitic character of the transition inevitably destroy any bcc single crystal when passing through the transition. However, Stassis *et al.* succeeded in growing a sufficiently large bcc single grain by cycling several times through the β-γ transition and first phonons of the transverse $T_1[\xi\xi 0]$ branch with $[1\bar{1}0]$ polarization have been published.[3]

The phonons in the fcc phase are dominated by a low-energy transverse $T[\xi\xi\xi]_{\rm fcc}$ branch. It is this transverse shuffling of the $(111)_{\rm fcc}$ planes which achieves partly the fcc-to-bcc transition. The corresponding phonon in the bcc phase is a transverse displacement of $(110)_{\rm bcc}$ planes. Indeed, the measurements of the $T_1[\xi\xi 0]_{\rm bcc}$ branch with $[1\bar{1}0]$ polarization in γ-La show phonons of similar low energy.[3] Such low frequencies for phonons have also been observed in the bcc phase of the group-IV metals.[4–6] In general, because of the similarity of the phase sequences in group-III and -IV metals, phonon dispersions in group-III bcc phases are expected to show similar low-

energy and anharmonic phonons as known for the bcc phases of the group-IV metals.

Here we report a complete measured phonon dispersion in γ-La. The problem of the martensitic phase transition has been overcome by growing single crystals from the melt *in situ* on the neutron spectrometer. We shall show the existence of particularly low and overdamped phonons which are related to the displacive phase transition and shall prove that in spite of the monoatomic structure these overdamped phonons have completely different intensities and line shapes in different but equivalent directions in reciprocal space.

II. EXPERIMENTAL DETAILS

High-purity La rods of 100 mm in length and 8 mm in diameter were prepared at the Ames Laboratory. Vacuum fusion analysis of the raw material yielded a dominant content of gaseous impurities in the order of 190 wt ppm oxygen, 130 wt ppm nitrogen, 1650 wt ppm hydrogen, and 35 wt ppm carbon. The samples were mounted by means of two Mo screws, but otherwise crucible free in the combined single-crystal growth and measurement furnace.[5,7] bcc single crystals of maximal 50 mm in length were grown *in situ* on the three-axis spectrometer by zone melting. The temperature of the sample was maintained above the transition temperature $T_{\gamma\beta}=1138$ K by passing an alternating current through the sample. In favorable cases temperature stability was of the order of ± 1 K over several days, but with a gradient of ± 5 K along the sample length. Absolute temperatures were calibrated with respect to the known $T_{\gamma\beta}$. Single crystals were grown and measured in a vacuum on the order of 10^{-6} mbar, and in order to minimize accumulation of impurities, a sample rod was never used twice.

In some cases the temperature dropped below the transition temperature. Cycling those samples 2–3 times through the transition usually resulted in the growth of *one* large grain of comparable size to the initially grown crystal.

Different crystals have been used with (100), (110), and (111) planes parallel to the scattering plane. All phonons have been measured in a constant final wave-vector k_f mode using thermal neutrons at the three-axis spectrometers IN8 and IN3 of the Institut Laue-Langevin and 1T of the Laboratoire Léon Brillouin. Because of the unusual large lattice parameter of γ-La, $a_{\rm bcc}=4.25$ Å, most of the measurements could be performed with $k_f=2.662$ Å^{-1} ($E_f=14.7$ meV) using graphite (002) monochromators and analyzers and a graphite filter to suppress $\lambda/2$ contributions. Typical horizontal collimations were 25′,40′,40′,40′.

III. PHONON DISPERSION AND ITS RELATION TO THE γ-TO-β TRANSITION

In spite of the high measuring temperatures and the small existence range of γ-La only 53 K below T_m, its phonon dispersion could be measured with high precision. Figure 1 shows the dispersion curves measured at 1163 K along the main symmetry directions and along the off-symmetry direction $[\xi\xi 2\xi]$. The measured frequencies are given in Tables I and II. The dispersion curves are very anisotropic; i.e., the $L[\xi\xi\xi]$ branch has a strong minimum at $\xi=\frac{2}{3}$ and the whole $T_1[\xi\xi 0]$ branch is of low energy. The $L\frac{2}{3}(111)$ and $T_1\frac{1}{2}(110)$ modes are connected via a valley of transverse low-energy phonons along $[\xi\xi 2\xi]$. All these low-energy phonons are strongly damped and are remarkably well described by a damped oscillator function [see Eq. (2)]. Consequences of this strong damping are illustrated by the solid circles representing phonon groups at $L\frac{2}{3}(111)$ in Fig. 1. Each of them represents the maximum of a scan in Q around $\mathbf{Q}=\frac{4}{3}(111)$ and in the [111] direction at a given energy transfer. These so-called constant-energy scans show an increasing intensity with decreasing energy transfer. At zero transfer, a maximum intensity is observed, apparently suggesting that the Brillouin-zone boundary in that direction is only $\frac{1}{3}$ of the value for bcc. Only scans in energy and at fixed $\mathbf{Q}$ (see Fig. 2) reveal the real character of this elastic intensity: Inelastic events are strongly damped, and the intensity of inelastic origin reaches down to zero energy transfer. However, the constant-energy scans around $L\frac{2}{3}(111)$ give us two important pieces of information: The position of the peak locates the minimum along $L[\xi\xi\xi]$ at $|Q|=1.340(2)$ rlu, i.e., slightly beyond the commensurate position $|Q|=\frac{4}{3}$, and the width of the peak full width at half maximum (FWHM)$\simeq 0.1$ rlu yields a correlation length for the collective propagation of the $L\frac{2}{3}(111)$ phonon in the order of 20 Å. Finally, we state that the dispersion of γ-La resembles very much those of the bcc phase of the group-IV metals.[4–6] In particular, similar ill-defined phonons are observed in these metals.

The set of eigenvectors of the $T_1[\xi\xi 0]$ and $T_1[\xi\xi 2\xi]$ branches contains all displacements needed for the displacive phase transitions we know in group-III and -IV metals and are therefore of particular interest.

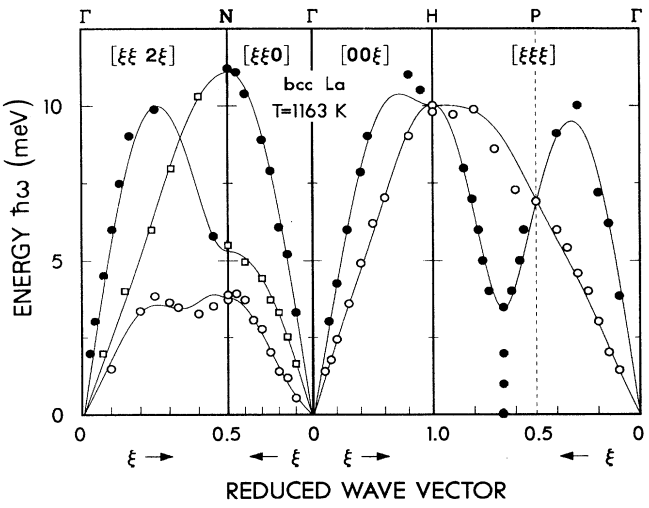

FIG. 1. Phonon dispersion for γ-La measured at 1163 K. The solid line shows a Born–von Kármán fit with force constants up to the fifth nearest-neighbor shell.

(i) The displacements of the transverse $T_1\frac{1}{3}(112)$ phonon are identical to that of the $L\frac{2}{3}(111)$ phonon. Out of three neighboring (111) planes, two oscillate against each other, whereas every third plane stays at rest. The ω-phase structure is then realized if the two planes collapse into each other.

(ii) The transverse zone-boundary phonon $T_1\frac{1}{2}(110) \equiv T_1\frac{1}{2}(112)$ displaces neighboring (110) planes in opposite $[1\bar{1}0]$ directions, thereby pushing the bcc(110) plane into the direction of the hcp *AB AB*... stacking sequence.

(iii) Two equivalent long-wavelength shears—for instance, $(1\bar{1}2)[\bar{1}11]$ and $(\bar{1}12)[1\bar{1}1]$—squeeze the bcc octahedron to a regular hcp or fcc one, thereby changing the angle from 109.5° to 120°. These shears are roughly those given by the initial slope of the transverse $[\xi\xi 2\xi]$ phonon branch with almost $[11\bar{1}]$ polarization (see Ref. 4).

(iv) Long-wavelength shears $(110)[1\bar{1}1]$, which correspond to the initial slope of the $T_1[\xi\xi 0]$ phonon branch, shift the bcc(110) planes toward a fcc *ABC ABC*... stacking sequence.

Figure 2 shows the neutron groups measured for the transverse $T_1[\xi\xi 0]$ and $T_1[\xi\xi 2\xi]$ phonon branches, and results of fits with the damped oscillator function are given in Table II. Already at low $q \simeq 0.1$ rlu the phonons

TABLE I. Phonons in γ-La at 1163 K; errors refer to statistical errors only.

$L[\xi\xi\xi]$		$T[\xi\xi\xi]$		$L[00\xi]$	
ξ	$\hbar\omega$ (meV)	ξ	$\hbar\omega$ (meV)	ξ	$\hbar\omega$ (meV)
0.1	3.85(5)	0.1	1.43(13)	0.134(22)	3
0.15	6.2(1)	0.15	2.03(12)	0.2	4.28(15)
0.2	7.2(1)	0.2	3.0(1)	0.287(22)	6
0.3	10.3(9)	0.25	4.0(1)	0.4	7.8(2)
0.4	9.1(6)	0.3	4.61(25)	0.460(24)	9
0.560(7)	6	0.35	5.4(1)	0.8	11(1.1)
0.58(1)	5	0.4	6.0(3)	0.9	10.5(5)
0.62(3)	4	0.5	6.9(3)		
0.67	3.5(1)	0.6	7.3(3)		
0.660(2)	2	0.7	8.6(7)		
0.660(2)	1	0.8	9.9(7)		
0.650(2)	0	0.9	9.7(7)		
0.730(24)	4	1	9.30(24)		
0.760(13)	5				
0.780(9)	6				
0.81(3)	7				
0.85(1)	8				

$T[00\xi]$		$L[\xi\xi 0]$		$T_{[001]}[\xi\xi 0]$	
ξ	$\hbar\omega$ (meV)	ξ	$\hbar\omega$ (meV)	ξ	$\hbar\omega$ (meV)
0.1	1.4(1)	0.1	3.3(1)	0.1	1.66(10)
0.15	1.8(1)	0.15	5.20(14)	0.15	2.52(10)
0.2	2.45(3)	0.2	6.10(17)	0.2	3.3(1)
0.3	3.6(1)	0.25	7.9(7)	0.25	3.74(10)
0.4	4.9(2)	0.3	8.9(2)	0.3	4.43(18)
0.5	6.2(4)	0.4	10.4(3)	0.4	4.96(17)
0.6	7.0(2)	0.45	11.1(2)	0.5	5.50(12)
0.8	9.0(5)	0.5	11.2(3)		
1	9.8(4)				

$L[\xi\xi 2\xi]$		$T_2[\xi\xi 2\xi]$	
ξ	$\hbar\omega$ (meV)	ξ	$\hbar\omega$ (meV)
0.028(30)	2	0.072(29)	2
0.046(30)	3	0.148(11)	4
0.075(49)	4.5	0.239(23)	6
0.104(30)	6	0.306(29)	8
0.130(49)	7.5	0.4	10.3(1.6)
0.164(24)	9		
0.200(24)	10.5		
0.25	9.9(1.5)		
0.45	5.8(1.2)		

TABLE II. Phonons in γ-La at 1163 K fitted with a damped-oscillator function.

$T_{[1\bar{1}0]}[\xi\xi 0]$			$T_1[\xi\xi 2\xi]$		
ξ	$\hbar\omega$	Γ (meV)	ξ	$\hbar\omega$ (meV)	Γ (meV)
0.1	0.8(1)	0.6(1)	0.1	1.47(10)	
0.15	1.19(9)	0.7(1)	0.2	3.4(1)	3.9(3)
0.2	1.7(1)	1.2(2)	0.25	3.9(2)	5.0(4)
0.25	2.0(1)	1.3(2)	0.3	3.6(2)	5.5(5)
0.3	2.8(1)	3.0(4)	0.33	3.5(1)	5.5(6)
0.35	3.1(2)	3.9(3)	0.4	3.3(2)	5.0(6)
0.4	3.7(2)	5.3(5)	0.45	3.5(2)	5.0(7)
0.45	3.9(4)	6.0(6)	0.5	3.7(2)	5.0(6)
0.5	3.9(4)	5.1(6)			

are quite broad, and close to the Brillouin-zone (BZ) boundary they are strongly damped ($\Gamma \geq \omega_0$). A weak but definitive maximum in the damping is found around $T_1\frac{1}{3}(112)$, i.e., for displacements toward the ω phase. This maximum in broadening correlates with a lowering of the fitted frequency. More surprisingly, the diffuse *elastic* intensity—the intensity on top of the phonons in Fig. 2—shows also a weak maximum around this so-called ω position. Whereas part of this diffuse elastic intensity is certainly due to elastic *incoherent* scattering,[8] any deviation from a smooth Debye-Waller behavior as a function of Q has to be of *coherent* origin. Whether the latter comes from static displacements around impurities[9] or is part of the structure factor and/or line shape of the overdamped excitations[10,11] remains a question of interpretation.

Whereas the phonon anomalies are very similar to those observed in the β phase of the group-IV metals, γ-La transforms upon cooling to a different close-packed structure. From the set of low-energy or large-amplitude fluctuations, the displacements corresponding to the fcc structure lock in at the transition temperature $T_{\gamma\beta}$. The transformation from bcc to fcc requires a change of the stacking sequence from *AB AB*... to *ABC ABC*... . These displacements cannot be achieved by short-wavelength or BZ boundary phonons, but only by *long-wavelength shears* as depicted in Fig. 3. For the bcc-to-fcc transition, the $(110)[1\bar{1}0]$ shears given by $C'=\frac{1}{2}(C_{11}-C_{12})$ perform the necessary elongations. This shear is given by the initial slope of the $T_1[\xi\xi 0]$ phonon branch. In a further step, the bcc octahedron has to be squeezed to a regular one. Similarly to the bcc-to-

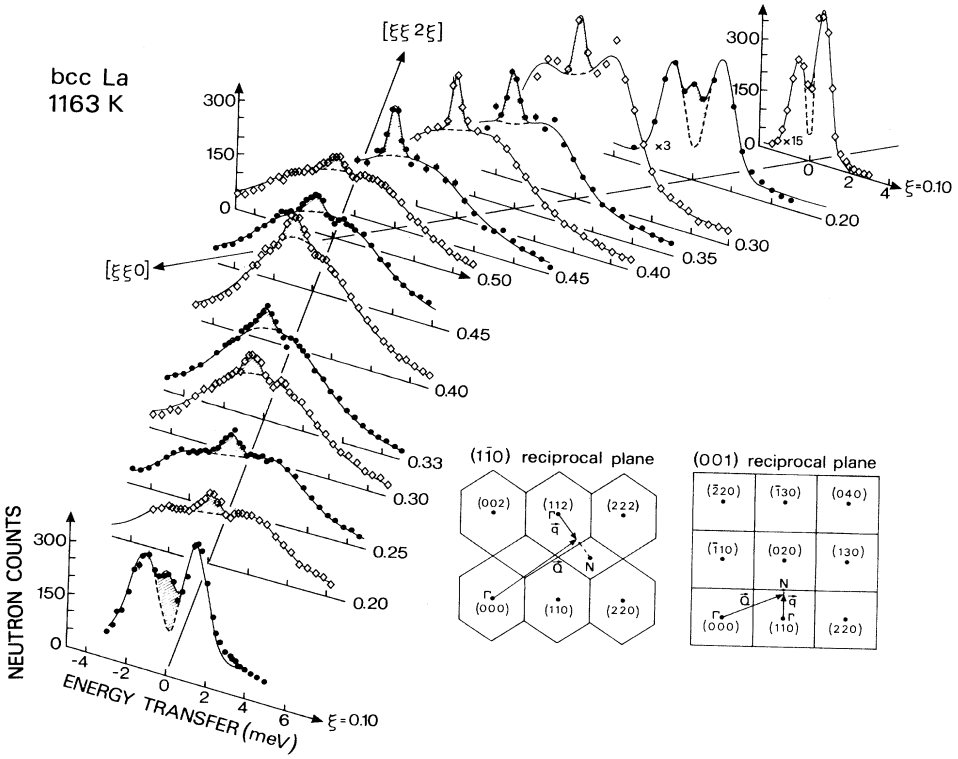

FIG. 2. Spectra of the $T_1[\xi\xi 2\xi]$ branch and of the $T_1[\xi\xi 0]$ branch in γ-La, measured in the $(1\bar{1}0)$ and (001) planes, respectively. The asymmetric intensity distributions in the spectra caused by varying $\lambda/2$ contamination has been taken into account in the fit function. Different crystals have been used, and better counting statistics has been achieved for the $T_1[\xi\xi 2\xi]$ branch. Energy resolutions (FWHM) are 0.8 and 0.7 meV for the $[\xi\xi 2\xi]$ and $[\xi\xi 0]$ directions, respectively. The solid lines show fits with a damped oscillator including a convolution with resolution. For the elastic intensity on top of the spectra, see text.

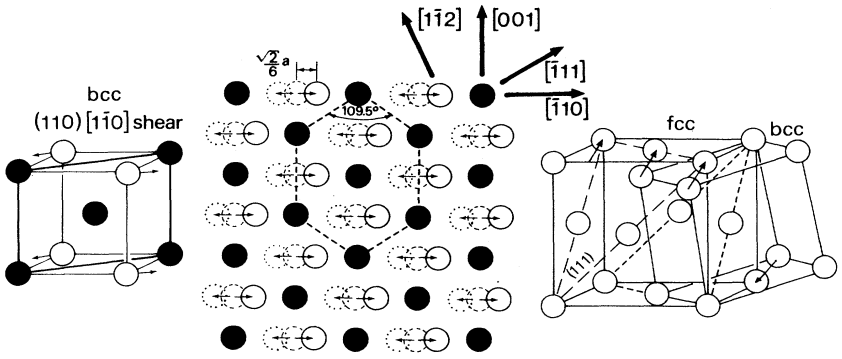

FIG. 3. Scheme of the bcc-to-fcc transition.

hcp transition, this can be achieved by two equivalent long-wavelength shears—for instance, $(1\bar{1}2)[\bar{1}11]$ and $(\bar{1}12)[1\bar{1}1]$—which are approximately given by C_-, i.e., the initial slope of the $[\xi\xi 2\xi]$ branch which has almost $[11\bar{1}]$ polarization.[4] This mechanism is analogous to the Burgers mechanism of the bcc-to-hcp transition, as both transitions preserve the interlayer distance and thus the repulsive effect of one layer with respect to the others. The essential difference is that in the case of the Burgers mechanism a BZ boundary phonon achieves the opposite shifts of two neighboring planes, whereas for the bcc-to-fcc transition two successive layers are shifted in the same direction which corresponds to a zone-center phonon or long-wavelength shear mode. Whereas for a BZ phonon its whole amplitude contributes to the shifting of adjacent planes, the displacement of adjacent planes due to long-wavelength shears remains infinitesimally small. The observation of low-energy or large-amplitude shear modes, as is the case in γ-La, does not therefore mean that the shear mode itself performs the displacements necessary for the transition, but only that the potential in the direction of the corresponding shifts is particularly flat.

The dominating role of C' is confirmed by thermodynamic considerations. Assuming no volume change through the γ-to-β transition, it can be shown that the local restoring forces tending to oppose the change to the fcc phase solely depend on the shear constant C';[12] i.e., a small C' alone indicates low potential barriers for a bcc-to-fcc transition.[13]

It is appealing to ask for a further softening of the phonons in the γ phase when the phase transition is approached. The temperature dependence of the $T_1[\xi\xi 0]$ branch has been investigated at 1143, 1163, and 1183 K. Line shapes and fitted frequencies stay the same within error bars.

The systematic behavior within the transition metals predicts for the group-III metals with only one d electron low restoring forces for a shearing of [111] chains against each other. The low-energy and strongly damped $L\frac{2}{3}(111)$ phonon in γ-La confirms this. This and its close resemblance to the $L\frac{2}{3}(111)$ phonons observed in the group-IV metals with two d electrons suggests that also La shows a tendency to transform to the ω structure. However, to our knowledge, no formation of the ω structure under pressure or alloying has been reported so far.

TABLE III. Interatomic force constants ϕ_{ij}^m in γ-La in units of N/m, obtained from a Born–von Kármán fit to the dispersion including five nearest-neighbor shells.

1_{xx}:3.288	1_{xy}:3.891	2_{xx}:4.131	2_{yy}:−1.991
3_{xx}:0.261	3_{zz}:−0.104	3_{xy}:−0.084	4_{xx}:−0.186
4_{yy}:0.119	4_{yz}:−0.058	4_{xy}:0.108	5_{xx}:−0.110
5_{xy}:−0.035			

IV. (QUASI)HARMONIC CALCULATIONS

To get a parametrization of the lattice dynamics, the dispersion curve shown in Fig. 1 was fitted by Born–von Kármán force constants ϕ_{ij}^m up to the fifth nearest-neighbor shell. The fit is shown as a solid line in Fig. 1, and the ϕ_{ij}^m are listed in Table III. Anharmonicity as evident from the damped phonons is not taken into account. As in our previous work,[4] the ϕ_{ij}^m's were used to calculate the phonon density of states, $Z(\omega)$ (Fig. 4), which in turn served to calculate the mean-square displacement $\langle u_x^2 \rangle$, Debye temperature Θ_D, and lattice entropy S_{vib}. For comparison, corresponding values of these quantities were calculated from the measured dispersion of the fcc

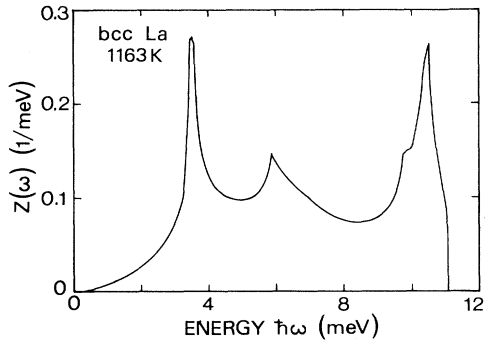

FIG. 4. Phonon density of state, $Z(\omega)$, for γ-La as calculated from the measured phonon dispersion.

TABLE IV. Debye temperature Θ_D, mean-square displacement $\langle u_x^2 \rangle$, lattice entropy S_{vib}, and the elastic constants C_{ij} for β- and γ-La.

	T (K)	Θ_D (K)	$\langle u_x^2 \rangle$ (Å^2)	S_{vib} (k_B/atom)	C_{11}	C_{12}	C_{44} (10^{12} dyn/cm^2)	$C'=\frac{1}{2}(C_{11}-C_{12})$
fcc La	295[a]	124	0.020	6.68	0.345	0.204	0.180	0.071
	660[a]	114	0.054	9.33	0.285	0.204	0.165	0.040
	1100[a]	106	0.102	10.97	0.294	0.245	0.162	0.025
	1138[b]			11.07				
bcc La	1138[b]			11.34				
	1163	89.1	0.154	11.40	0.310	0.290	0.103	0.010
	1163[c]				0.33	0.29	0.094	0.021

[a] Calculated from phonon measurements by Stassis *et al.* (Refs. 1 and 2).
[b] Extrapolated to $T_{\gamma\beta}$.
[c] Determined from initial slope of the corresponding phonon branch.

phase.[1,2] Elastic constants have been calculated from the force constants according to the formula derived by Squires[14] and alternatively directly from the measured initial slopes of the corresponding phonon branches. All values are listed in Table IV. The change in $\langle u_x^2 \rangle$ and Θ_D shows the softening of the bcc lattice with respect to the fcc lattice. This softening is very anisotropic; the bulk modulus $C^+=\frac{1}{3}(C_{11}+2C_{12})$ stiffens, whereas the shear moduli C_{44} and C' soften considerably.

Based on the phonon measurements at the corresponding temperatures in the β (Refs. 1 and 2) and γ phases, the vibrational entropy S_{vib} can be calculated in the quasiharmonic approximation, thereby permitting a quite reliable estimate of the vibrational excess entropy ΔS_{vib} at the β-to-γ transition. The temperature dependence of S_{vib} is shown in Fig. 5. We see from this figure that an harmonic extrapolation of S_{vib} to higher temperature fails because of the explicit temperature dependence of the phonon frequencies. Taking into account the temperature dependence of the phonons, we find $\Delta S_{vib}=0.27k_B$/atom. A comparison with the known excess enthalpy at the β-to-γ transition, $\Delta S_{tot}=0.32k_B$/atom,[15] shows that, similar to what has been found in the group-IV metals, the γ phase is primarily stabilized by an increase in *vibrational* entropy. The latter is dominated by the low-energy transverse phonons. The remaining difference $\Delta S_{tot}-\Delta S_{vib}=\Delta S_{el}$ can then be ascribed to the difference in electronic entropy.

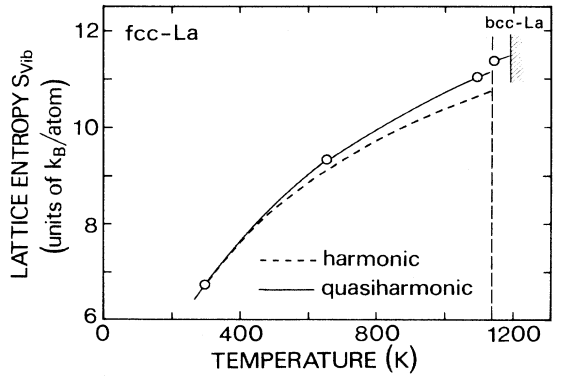

FIG. 5. Lattice vibrational entropy S_{vib}(○) for β-La calculated from $Z(\omega)$ determined at the corresponding temperature (Refs. 1, 2, and this work): harmonic extrapolation of S_{vib} based on $Z(\omega)$ at 295 K (dashed line) and second-order polynomial fit (solid line).

V. SYMMETRY-BREAKING PHONONS

It is evident from Fig. 2 that the transverse phonons along the $[\xi\xi 2\xi]$ and $[\xi\xi 0]$ directions are strongly damped. Close to or at the BZ boundary, the lifetimes of these excitations are only of the order of a few vibrational periods. Phonon-phonon interactions can be seen as the physical origin of these short lifetimes; in a first approxi-

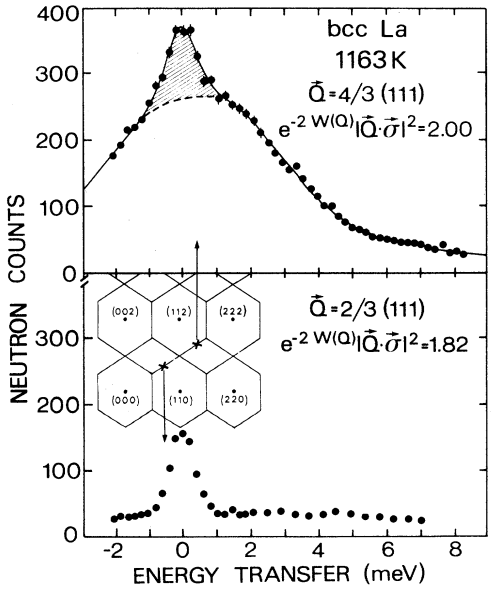

FIG. 6. $L\frac{2}{3}(\xi\xi\xi)$ phonon measured at two different but equivalent points in reciprocal space. For both scans k_f(fix)=2.662 Å^{-1} with a collimator of 25′,40′,40′,40′ yielding an energy resolution (FWHM)≃0.8 meV has been chosen. The prefactor of the one-phonon scattering is almost equal for both positions. For the fit procedure, see Fig. 2.

mation, one-phonon events decay into two or more phonons and, vice versa, multiple-phonon excitations combine to one phonon. Interference effects due to this multiple-phonon creation and annihilation have been observed and discussed in the quantum solid ^{4}He.[16,17] In a theory reviewed by Glyde,[18] alterations of the one-phonon cross section $S_j(Q,\omega)_{1\text{ phonon}}$ are expressed in terms of the observed damping $\Gamma_j(\mathbf{q})$:

$$S_j(Q,\omega)_{\text{interf}}=S_j(Q,\omega)_{1\text{ phonon}}\{1+A(\mathbf{Q},\mathbf{q})+B(\mathbf{Q},\mathbf{q},\omega,\omega_j(\mathbf{q}),\Gamma_j(\mathbf{q}))\}\ . \tag{1}$$

A first contribution A alters the one-phonon intensity for apparently equivalent loci in reciprocal space, and a further contribution B affects the one-phonon line shape itself. In summary, the observation of strong damping in γ-La motivates the search for further effects of anharmonicity, namely, pronounced alterations of the one-phonon scattering law.

For a monoatomic Bravais lattice, as is the case for γ-La, the one-phonon scattering law of the jth phonon branch may be written as[19]

$$S_j(Q,\omega)_{1\text{ phonon}}=\frac{b^2}{M}|\mathbf{Q}\cdot\boldsymbol{\sigma}_j(\mathbf{q})|^2 e^{-2W(Q)}\frac{\hbar\omega}{(1-e^{-\hbar\omega/k_BT})}\frac{1}{\pi}\frac{\Gamma_j(\mathbf{q})}{\hbar^2[\omega^2-\omega_j^2(\mathbf{q})]^2+\omega^2\Gamma_j^2(\mathbf{q})}\ . \tag{2}$$

b and M are the coherent scattering length and atomic mass of the element, respectively, $\boldsymbol{\sigma}_j(\mathbf{q})$ is the q-dependent eigenvector or polarization of the jth phonon branch. In harmonic approximation the Debye-Waller factor $e^{-2W(Q)}=e^{-\langle u_x^2\rangle Q^2}$. Separating the Q-dependent prefactor $e^{-2W(Q)}|\mathbf{Q}\cdot\boldsymbol{\sigma}_j(\mathbf{q})|^2$, the remaining response function gives the phonon line shapes as a function of energy. Here the response function has been written in the form of a damped oscillator. For vanishing damping $\Gamma\to 0$, it has to be replaced by two δ functions centered at $\pm\omega_j(q)$. By means of the results of the previous section, the prefactor can be calculated and phonons, measured at different but equivalent places in reciprocal space, can be compared directly.

Alterations of this one-phonon scattering law due to phonon-phonon interaction are explicitly expressed in terms of the damping [Eq. (1)]. Therefore these effects should be strongest along those phonon branches, where the damping is observed. Figures 6–8 show a series of such phonons measured—according to the one-phonon scattering law—at equivalent points in reciprocal space.

Scans of the $L\frac{2}{3}(111)\equiv T_1\frac{1}{3}(112)$ phonon measured in two different BZ's are compared in Fig. 6. The prefactor varies between the two positions by only 10% (see inset). Whereas at $\mathbf{Q}=\frac{2}{3}(111)$ no phonon intensity emerges out of the background, inelastic intensity with the characteristic line shape of an overdamped phonon is clearly visible at $\mathbf{Q}=\frac{4}{3}(111)$. Both measurements have been performed with the same spectrometer configuration, and variations in the resolution volume are therefore negligible.

In a further step, Fig. 7 compares the whole transverse phonon branch $T_1[\xi\xi 2\xi]$ measured along two different but equivalent directions in the (112) BZ. Considerable variations of the scalar product $|\mathbf{Q}\cdot\boldsymbol{\sigma}|$ (see inset) render a direct comparison of the measurements in the direction of $\mathbf{Q}=(1-\xi,1-\xi,2+2\xi)$ with those in the direction of $\mathbf{Q}=(1+\xi,1+\xi,2-2\xi)$ difficult, even though a clear tendency of an almost complete loss of intensity for measurements in the direction of $\mathbf{Q}=(1-\xi,1-\xi,2+2\xi)$ is discernible. Already at $\xi=0.1$ where the prefactors differ by 20% for the two directions the phonon intensities differ by 60%; at $\xi=0.2$, the prefactors differ by 64%, but the phonon intensity is only visible in the direction of $\mathbf{Q}=(1+\xi,1+\xi,2-2\xi)$. For $\xi=0.5$, changes in the pre-

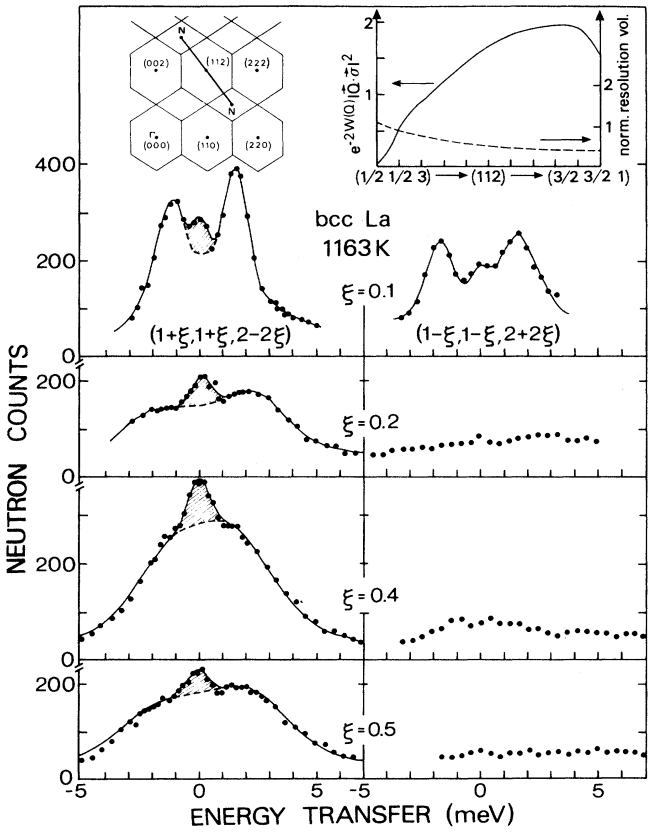

FIG. 7. Comparison of $T_1[\xi\xi 2\xi]$ phonons measured in the (112) BZ, but in two different directions. Variations of the prefactor for the one-phonon scattering and those of the resolution volume are shown in the inset. Same spectrometer set up as in Fig. 6.

factor are so drastic that a comparison of phonon intensities is no longer possible.

To overcome the strong variations of the prefactor, the $T_1[\xi\xi\, 2\xi]$ branch has also been measured in the (222) BZ where the variation of the prefactor is less important (see inset of Fig. 8). This has to be payed by a considerable loss in energy resolution imposed by the use of a shorter neutron wavelength. For $\xi=0.33$, i.e., at the point where $T_1\frac{1}{3}(112)\equiv L\frac{2}{3}(111)$, the prefactors are identical in both directions, but the phonon intensity measured at $\mathbf{Q}=(\frac{8}{3}\,\frac{5}{3}\,\frac{5}{3})$ is only half of that measured at $\mathbf{Q}=(\frac{4}{3}\,\frac{7}{3}\,\frac{7}{3})$. At the two N points, the prefactors differ by a factor of 2.8 and the measured intensity differences are comparable to this value. A more precise determination is not possible because the background counting, i.e., the base line, is not exactly known. Within these uncertainties the phonon intensities for the two N points are, with the exception of the trivial prefactor, identical.

As shown by Ambegaoker, Conway, and Baym,[20] the first-moment sum rule

$$\int_{-\infty}^{\infty} S_j(\mathbf{Q},\omega)_{\text{interf}}\omega\frac{d\omega}{2\pi}=e^{-2W(Q)}\frac{\hbar|\mathbf{Q}\cdot\boldsymbol{\sigma}_j(q)|^2}{2M} \tag{3}$$

remains valid when interference is present. Even though an experimental verification of the sum rule is complicated by the necessary integration over large ω ranges, the phonon groups shown in Fig. 6 indicate a violation of this rule. An explanation is probably related to the fact that damping is so strong at the ω point, and therefore interference terms higher than of first order have to be taken into account.

Another rule of the interference scattering between one and multiple phonons appears, however, to be fulfilled. In the approximation used by Glyde,[16] it can be shown that at Q lying midway between two reciprocal lattice points the different interference terms cancel; i.e., phonon spectra measured at these points in different BZ's are identical. The two N-point phonons shown in Fig. 8 indicate indeed equal phonon intensity—when corrected for the prefactor.

How do these observations compare with the earlier measurements on bcc ^{4}He (Refs. 16 and 17)? Also, in solid He, broadened and asymmetric phonon line shapes are observed for scattering processes in the $(1\bar{1}0)$ plane and integrated intensities strongly vary as a function of $|Q|$ around the one-phonon prefactor $e^{-2W(Q)}|\mathbf{Q}\cdot\boldsymbol{\sigma}|^2$. Compared to γ-La, the broadening in solid He is less pronounced and consequently intensity alterations are not as drastic as in γ-La (see, for instance, Fig. 6). Both systems transform to a densely packed structure and low-energy and short-lived phonons are the signature of strongly anharmonic potentials with low barriers for the displacive transition.

Differences between both systems have to be noted: (i) Within the $(1\bar{1}0)$ scattering plane, the intensity variations in solid He scale with $|Q|$ and are independent of the direction of $\mathbf{Q}$. This cannot be confirmed in γ-La. For instance, the left and right half of Fig. 8 refer to identical $|Q|$, but different $\mathbf{Q}$. (ii) In solid He no violations of the sum rule [Eq. (3)] are observed for the transverse $T_{[1\bar{1}0]}[\xi\xi 0]$ phonon branch. In γ-La this branch is strongly damped when measured in the (110) BZ as in Fig. 2. Probably, one does therefore observe intensity variations for this branch in different BZ's. Corresponding measurements are yet missing. (iii) It is argued that the anharmonic vibrations in solid He are related to its large zero-point motion and its low Debye-Waller factor [$\Theta_D\simeq 22.5$ K (Refs. 16–18)]. Both explanations fail in γ-La: Neither zero-point motions are large nor is the Debye temperature extremely low (see Table IV). Rather, its particular electronic configuration—one d electron, unoccupied f shell—is the origin of the extremely anharmonic potential.

So far, interference effects have been discussed for anharmonic quantum crystals such as ^{4}He. They have also been observed in simple metals such as potassium.[21] The reported intensity and line-shape variations of the

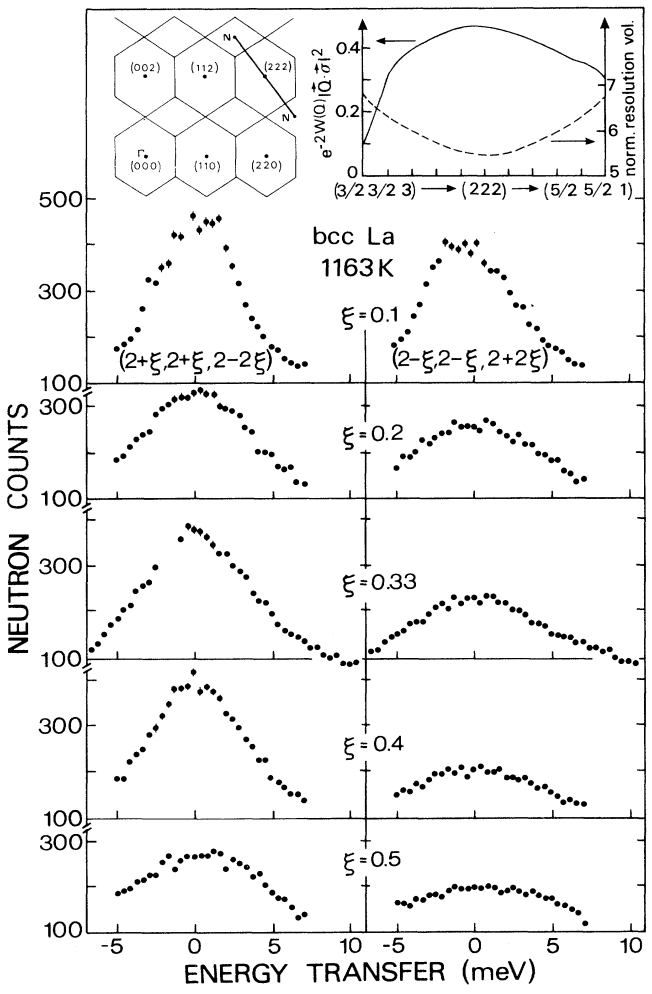

FIG. 8. Similar to Fig. 7, but measurements are now in the (222) BZ. Variations of the prefactor for the one-phonon scattering and those of the resolution volume are shown in the inset. Now $k_f(\text{fix})=3.86$ Å^{-1} with an energy resolution of 2.8 meV. Note that the intensity scale starts at a background level of 100 counts.

one-phonon scattering law are small when compared to γ-La and bcc ^{4}He. The reason is that the damping, i.e., the anharmonicity, is so much more pronounced in the hitherto not accessible bcc phases of the group-III and -IV metals.

These bcc phases can be stabilized at room temperature through alloying with other transition metals. The best-known example is $Zr_{1-x}Nb_x$. Indeed, strong violations of the one-phonon scattering law have been observed in the bcc phase of this alloy ($x=0.2$) by Axe, Keating, and Moss[22] and more recently by Noda, Yamada, and Shapiro.[23] Very broad and ill-defined phonon groups along $T_1[\xi\xi 2\xi]$ were measured and intensity and line-shape variations at equivalent points in Q space similar to the one in γ-La were reported. The authors explain the anomalies by a local symmetry breaking due to a coexisting ω phase.[24] In view of the present results in *pure* γ-La, it seems likely that in the $Zr_{1-x}Nb_x$ ($x=0.2$) system the observed phonon anomalies are genuine to a crystal with strongly anharmonic vibrations rather than an effect of heterophase fluctuations.

Recent molecular-dynamic calculations of the dynamical response of pure bcc Zr by Wang, Ho, and Harmon[25] support this view. Simulating the total inelastic-scattering law $S(Q,\omega)_{\text{tot}}$, i.e., the sum over *all* interference and multiple-phonon processes at a given **Q**, they predict line-shape and phonon anomalies similar to those measured in γ-La. In particular, they calculate a damping of the ω phonon at $\mathbf{Q}=\frac{4}{3}(111)$ as strong as observed in γ-La and predict that this same phonon shows at $\mathbf{Q}=\frac{2}{3}(111)$ less damping and only 5% of the peak intensity of that at $\mathbf{Q}=\frac{4}{3}(111)$. Qualitatively, they also confirm that the phonon intensity around $\mathbf{Q}=(1+\xi, 1+\xi, 2-2\xi)$ and $\mathbf{Q}=(2+\xi, 2+\xi, 2-2\xi)$ is less intense for $\xi<0$ than for $\xi>0$.

VI. CONCLUSIONS

The phonon dispersion of γ-La is dominated by low-energy transverse phonons along $[\xi\xi 2\xi]$ and $[\xi\xi 0]$, giving rise to a pronounced asymmetry in the vibrational behavior. The eigenvectors of these low-energy phonons are in the directions of the displacements needed for close-packed low-temperature structures. These phonons are strongly damped and have close to the BZ-boundary lifetimes of the order of one to a few vibrational periods. As concluded from the weak dispersion of these phonon branches toward the BZ boundary, they have a localized character for directions perpendicular to [111]. All this is characteristic of a more sluggish and fluctuative motion than for long-range periodic phonon propagation.

This weakness of the lattice potential for displacements toward close-packed structures is genuine to γ-La and indicative for the transformation to a close-packed structure. Via its contribution to the lattice entropy, these low-energy excitations are also the main reason to stabilize the open bcc structure at high temperature.

Because these phonons are so heavily damped, interference effects due to phonon-phonon interaction strongly alter the one-phonon scattering law. This may explain the different phonon responses at equivalent points in reciprocal space where in alloyed samples of similar bcc phases (*Zr*Nb, *Zr*Co, *Zr*O) elastic diffuse scattering is observed.[26,9] In analogy to the explanation of this elastic diffuse scattering by static displacements of the bcc lattice toward the low-temperature structures, the here-discussed *inelastic* diffuse scattering is characteristic of *dynamical* fluctuations toward the low-temperature structures. More precisely, the probability distribution of a given atom around its equilibrium position no longer oscillates harmonically, but is strongly anisotropic. The density distribution itself distorts during the motion. The elementary excitation has to be viewed as a coupled mode: Purely displacive modes admix with other modes that accommodate the distortions generated by the displacements [see also Refs. 16 and 17]. Formally, this process is associated with the decay of one phonon into two and more phonons.[18]

Phonon line shapes have been analyzed by a damped oscillator. Calculations of the line shape via Eq. (1) go beyond this approach. Probably more precise intensity distributions will be generated by molecular-dynamics calculations.[25] Lattice potentials of γ-La suitable for both approaches have yet to be generated.

Phonon anomalies in γ-La resemble very much those observed in the bcc phases of the other group-III and -IV metals. Phonon damping for these metals is as strong as in γ-La. It is therefore very likely that similar deviations from the one-phonon scattering are present in these metals as well.

ACKNOWLEDGMENTS

We thank C. Z. Wang, K. M. Ho, and B. N. Harmon for communicating the results of their molecular-dynamic simulations prior to publication and for fruitful discussions about symmetry-breaking phonons. B. Gooding showed us how C' dominates the energy barrier tending to oppose the γ-to-β transition. Financial support by the Bundesministerium für Forschung und Technologie, Germany, under Contract No. 03-HE2MUE-0 is gratefully acknowledged. Ames Laboratory is operated for the U.S. Department of Energy by Iowa State University under Contract No. W-7405-Eng-82. This work was supported by the Director for Energy Research, Office of Basic Energy Sciences.

[1]C. Stassis, C.-K. Loong, and J. Zarestky, Phys. Rev. B **26**, 5426 (1982).

[2]C. Stassis, G. S. Smith, B. N. Harmon, K.-M. Ho, and Y. Chen, Phys. Rev. B **31**, 6298 (1985).

[3]C. Stassis and J. Zarestky, Solid State Commun. **52**, 9 (1984).

[4]W. Petry, A. Heiming, J. Trampenau, M. Alba, C. Herzig, H. R. Schober, and G. Vogl, Phys. Rev. B **43**, 10 933 (1991).

[5]A. Heiming, W. Petry, J. Trampenau, M. Alba, C. Herzig, H. R. Schober, and G. Vogl, Phys. Rev. B **43**, 10 948 (1991).

[6]J. Trampenau, A. Heiming, W. Petry, M. Alba, C. Herzig, W. Miekeley, and H. R. Schober, Phys. Rev. B **43**, 10 963 (1991).

[7]Th. Flottmann, W. Petry, R. Serve, and G. Vogl, Nucl. In-

strum. Methods A **260**, 165 (1987).
[8]$\sigma_{inc} = 1.1$ barn.
[9]A. Heiming, W. Petry, G. Vogl, J. Trampeneau, H. R. Schober, J. Chevrier, and O. Schärpf, Z. Phys. B **85**, 239 (1991).
[10]W. C. Kerr, A. M. Hawthorne, R. J. Gooding, A. R. Bishop, and J. A. Krumhausl, Phys. Rev. B **45**, 7036 (1992).
[11]P. A. Lingård, J. Phys. IV, Colloq. C4, Suppl. J. Phys. III, **1**, C4-3 (1991).
[12]R. J. Gooding (private communication).
[13]We actually measured a volume contraction of 3% for fcc La compared to bcc La when running through the γ-to-β transition. The additional homogeneous strain due to this volume contraction is about 3% of the shear strain involved in the bcc-to-fcc transition and therefore plays no crucial role in the evaluation of the local restoring forces.
[14]G. L. Squires, in *Proceedings of the Symposium on Inelastic Scattering of Neutrons in Solids and Liquids,* Chalk River, edited by S. Eklund (IAEA, Vienna, 1963), Vol. II, p. 71.
[15]R. Hultgren, P. D. Desai, D. T. Hawkins, M. Gleiser, K. K. Kelly, and D. D. Wagman, *Selected Values of the Thermodynamic Properties of the Elements* (American Society for Metals, Metals Park, OH, 1973).
[16]E. B. Osgood, V. J. Minkiewicz, T. A. Kitchens, and G. Shirane, Phys. Rev. A **5**, 1537 (1972).
[17]V. J. Minkiewicz, T. A. Kitchens, G. Shirane, and E. B. Osgood, Phys. Rev. A **8**, 1513 (1973).
[18]H. R. Glyde, Can. J. Phys. **52**, 2281 (1974).
[19]B. Dorner, *Coherent Inelastic Neutron Scattering in Lattice Dynamics,* Springer Tracts in Modern Physics Vol. 93 (Springer Verlag, Berlin, 1982).
[20]V. Ambegaokar, J. M. Conway, and G. Baym, in *Lattice Dynamics,* edited by R. F. Wallis (Pergamon, New York, 1965), p. 261.
[21]J. Meyer, G. Dolling, R. Scherm, and H. R. Glyde, J. Phys. F **6**, 943 (1976).
[22]J. D. Axe, D. T. Keating, and S. C. Moss, Phys. Rev. Lett. **35**, 530 (1975).
[23]Y. Noda, Y. Yamada, and S. M. Shapiro, Phys. Rev. B **40**, 5995 (1989).
[24]For the work by Noda, Yamada, and Shapiro (Ref. 23), the coexistence of the ω phase is static because of quenching to room temperature. The measurements of Axe, Keating, and Moss (Ref. 22) have been performed at 1238 K in the single bcc phase, and the ω phase due to alloying is supposed to be quasistatic.
[25]C. Z. Wang, K. M. Ho, and B. N. Harmon (unpublished).
[26]S. C. Moss, D. T. Keating, and J. D. Axe, in *Phase Transformations,* edited by L. E. Cross (Pergamon, Oxford, 1973), p. 179.